Adaptive Fast Fixed-time Sliding Mode Control For Uncertain Robotic Manipulators

Xin Zhang* and Shaojun Qing

School of Automation and Electrical Engineering of Lanzhou Jiaotong University, Lanzhou, 730070, China

Corresponding author. E-mail: zhangx@mail.lzjtu.cn

Received: October 14, 2023; Accepted: December 10, 2023

In this paper, a novel adaptive terminal sliding mode (TSM) control method is suggested for the operation and adjustment of uncertain robots under the influence of internal parameter errors and external perturbations. Firstly, a novel TSM surface was designed with the aim of achieving continuous and smooth output torque while ensuring rapid convergence of tracking error. Secondly, the TSM is combined with adaptive control, and an adaptive mechanism is utilized to determine these unknown upper bounds, in order to implement accurate trajectory control in the existence of unknown lumped disturbance. The Lyapunov stability theory is utilized to prove global fixed-time stability, ensuring that the state of the system converges to the origin in fixed time. Importantly, the proposed scheme offers the advantage of continuous and transient-free control torque, eliminating undesired vibrations and ensuring smoother control torques that are well-suited for practical applications. Finally, the simulation experiments unequivocally establish the efficacy and superiority of the controller that was devised.

Keywords: Robot manipulator; Sliding mode control; Adaptive control; Trajectory tracking; Fixed time convergence

http://dx.doi.org/10.6180/jase.202411_27(11).0005

1. Introduction

Manipulator trajectory control is an important application in industrial automation. As a time-varying nonlinear system with parameter uncertainty and external disturbance, the manipulator is affected by factors such as sensor noise, friction, and payload variations. In order to overcome these challenges and achieve high-precision trajectory control, rapid response, real-time obstacle detection and avoidance, various control schemes have been used to control manipulators for specific operational tasks, such as PID [1], Fuzzy algorithm [2], Neural Network [3–5], Backstepping control [6–8] and Sliding mode control (SMC). SMC has garnered significant interest among researchers in the field of nonlinear system control, owing to its impressive benefits such as rapid response, immunity to changes in parameters, and resilience against external disruptions.

In the previous analysis of linear SMC, it was found that the system state takes an infinite amount of time to reach the equilibrium point. This observation implies the need for further research on the optimization of control systems for faster convergence. In order to achieve this objective, scholars have introduced terminal SMC (TSMC) which strives for finite-time convergence of the system's state trajectory. For example, references [9–13] propose a TSMC methodology for uncertain nonlinear systems, ensuring finite-time convergence of the system's state to the origin. Geng et al. [14] proposed a method to introduce time-varying gains in nonsingular TSMC (NTSMC), which improves the speed of convergence of the system and reduces the control input. Compared to the conventional super-twisting control strategy involving time delay estimation, a robust adaptive double-layer SMC (ADLSMC) approach was proposed in [15]. This approach is capable of

achieving dynamic trajectory tracking. References [16–18] proposed a terminal sliding mode control algorithm that guarantees rapid convergence of the system in the direction of any starting state to the sliding surface and equilibrium point. In Mobayen et al. [19], an adaptive SMC technique with super-twisting algorithm is used to make the tracking error with finite time convergence.

However, a disadvantage of utilizing finite-time control is that it relies on the initial parameters of the system to dictate the convergence time. To address this issue, researchers have put forward the implementation of fixed-time control technology. As compared to finite-time control, it enables the system to reach stability within a predetermined amount of time that is irrespective of the initial conditions. Thus, fixed-time has been extensively applied in diverse non-linear control applications. In their proposal, Zhang et al. [20] put forward a novel fixed-time TSM approach that guarantees precise route control for vessels amidst external disturbances in the ocean. To attain precise and rapid tracking capabilities, a novel SMC technique was proposed by [21]. This method not only eliminates singularity issues entirely, but can also be implemented directly in a multi-joint robot system. A model-free control approach is proposed in [22, 23], which combines the use of TSMC with time delay techniques. Hu et al. [24] developed a SMC with fixed time characteristics and estimated the uncertainty in the system through neural networks, and finally solved the problem of saturating the input of the robot controller by using an inverse tangent function. In this regard, although the problem of convergence time has been solved in the above research. However, these solutions are based on the known upper bound of system uncertainty or disturbance observer. In reality, as a result of the unpredictability and intricacy of non-linear systems, the implementation of these technologies may pose more difficulties and room for debate. Zhang et al. in [25, 26] proposed a robust TSMC for robotic arm tracking problem combined with adaptive technology. The uppermost thresholds of indeterminacy and exterior disruptions can be assessed via an adaptive parameter tuning technique.

In addition to the above issues, the chattering of the SMC needs to be addressed. An innovative adaptive TSMC technique is introduced in [27] that allows the system to attain uninterrupted control output for the objective. Thus, it effectively eradicates chattering without compromising robustness. In [28, 29], a second-order TSM scheme is proposed to mitigate chattering by integrating the control input. In the control of uncertain robots to track trajectories, the TSMC method suggested in [30, 31] can guarantee smooth and stable control torque, ensuring speedy convergence of tracking error for the system. To improve robustness and eliminate chattering, super-twisting sliding mode algorithms were utilized for trajectory tracking in previous studies [32–34]. Sai et al. [35] constructed an adaptive nonsingular SMC method to assure the system achieves convergence within a predetermined duration. In addition, he developed an actuator saturation compensator, which compensated the controller with faster trajectory tracking rate and less joint jitter. These algorithms offer efficient solutions in achieving desired tracking performance.

Drawing on the preceding discourse, this paper presents a trajectory tracking control technique suited for uncertain robotic systems. This approach is notable for its rapid convergence, exceptional steady-state tracking precision, and absence of chattering. This study mainly studies the following aspects : (i) In contrast with the present TSMC approach [9–19], our presented control strategy displays a convergence duration unaffected by the incipient state of the system, enabling it to be obtained beforehand, henceforth achieving fixed-time convergence. (ii) Compared with [10, 16, 18, 27], by introducing the continuous segmentation function into the sliding mode surface, it not only realizes the continuity and nonsingularity of the SMC, but also helps by suppressing the jitter phenomenon in the control input. Furthermore, it ensures an enhanced convergence rate of the system states when deviating from the equilibrium state. (iii) Different from the method in [14, 17, 18, 21, 30, 31], the adaptive technique designed in this paper can adjust the parameters automatically according to the state of system, thus solving the problem of needing to know the upper bound of the system's composite uncertainty term beforehand in [14, 17, 18, 21, 30, 31]. Finally, compared to the methods described in [16], [17] and [21], this approach exhibits greater robustness against uncertainties and achieves faster convergence.

This article is structured into the subsequent segments: In section 2, the problems that need to be solved are introduced, and the required mathematical model is proposed. In section 3, we introduce the adaptive nonsingular fast TSMC (ANFTSMC) design and verify and analyze its stability. Section 4 validates the proposed methodology through simulation and compares it to the existing techniques. Section 5 concludes by summarizing the preceding research outlined in this paper.

2. Theory and formula

2.1. Concept Explanation

There is a non-linear system that can be described as follows

$$x(t) = f(x), x(0) = x_0 \tag{1}$$

Where $x \in R^n$ is the state variable of the system, and $f(0) = 0.f(x)$ is a continuous nonlinear function in an area that is open near the origin. If the time for convergence is limited by a finite function $T(x_0)$, the system is considered to be fixed time stable. Put differently, the system can reach convergence within certain predetermined time constants represented by $T_{\max}$, with $T_{\max}$ being a constant that satisfies $T(x_0) < T_{\max}$.

Lemma 1 If a continuously bounded radial function $V(x)$ exists such that

$$\dot{V}(x) \leq -k_1 V^{\alpha}(x) - k_2 V^{\beta}(x) \tag{2}$$

Where $k_1 > 0, k_2 > 0, \alpha > 1, 0 < \beta < 1$. The system (1) complies with global fixed-time stability throughout the control process, of which the time T required to reach the equilibrium point satisfies

$$T \leq \frac{1}{k_1(\alpha - 1)} + \frac{1}{k_2(1 - \beta)} \tag{3}$$

Lemma 2 [25] Assuming that there exists a continuous function $V(x)$ that is always greater than zero for system (1). We can get

$$\dot{V}(x) \leq -a_1 V(x) - \left(a_2 V^{a_1}(x) + a_3 V^{b_2}(x)\right)^c \tag{4}$$

Where $a_1 > 0, a_2 > 0, a_3 > 0, b_1 c > 1, 0 < b_2 c < 1$. The time T, which needs to be procured by the system in order to attain a steady state complies with

$$\begin{aligned} T \leq & \frac{1}{a_1(b_1 c - 1)} \ln\left(1 + \frac{a_1}{a_2^c}\right) \\ & + \frac{1}{a_1(1 - b_2 c)} \ln\left(1 + \frac{a_1}{a_3^c}\right) \end{aligned} \tag{5}$$

Lemma 3 For any $\xi_1, \xi_1, \cdots, \xi_1 \geq 0$, the following inequalities satisfy

$$\sum_{i=1}^{N} \xi_i^p \geq \left(\sum_{i=1}^{N} \xi_i\right)^p \quad 0 < p < 1 \tag{6}$$

$$\frac{d}{dt}\left(\mathrm{sig}(x)^{\alpha}\right) = \alpha \dot{x} |x|^{\alpha - 1} \quad \alpha \geq 1 \tag{7}$$

Lemma 4 To facilitate future design work, we have established the following formula for ease of use.

$$\mathrm{sig}(x)^{\alpha} = |x|^{\alpha} \mathrm{sign}(x) \tag{8}$$

$$\frac{d}{dt}\left(\mathrm{sig}(x)^{\alpha}\right) = \alpha \dot{x} |x|^{\alpha - 1} \quad \alpha \geq 1 \tag{9}$$

2.2. Dynamic model of rigid manipulator

The dynamic equations of a multi-joint rigid robotic arm are given by

$$M(q)\ddot{q} + C(q, \dot{q})\dot{q} + G(q) = \tau + \tau_d \tag{10}$$

Where $q \in R^n$ is the joint position, $\dot{q} \in R^n$ and $\ddot{q} \in R^n$ represent the velocity and acceleration vectors, $M(q) \in R^{n \times n}$ is the inertial matrix, $C(q, \dot{q}) \in R^{n \times n}$ is the centrifugal and coriolis matrix, $G(q) \in R^n$ is the gravity term, $\tau \in R^n$ is the control torque, and $\tau_d \in R^n$ represents bounded external interference.

Given the difficulty in obtaining the complete model parameters of a manipulator in practical applications, a nominal parameter model of the manipulator is typically used. Hence, other than the unknown disturbance that impacts the trajectory control capability of manipulator systems, the model's parameter error is also a crucial factor that affects it. The expression of parameter uncertainty is as follows

$$\begin{cases} M(q) = M_0(q) + \Delta M(q) \\ C(q, \dot{q}) = C_0(q, \dot{q}) + \Delta C(q, \dot{q}) \\ G(q) = G_0(q) + \Delta G(q) \end{cases} \tag{11}$$

Where $M_0(q), C_0(q, \dot{q})$ and $G_0(q)$ are the nominal model parameters, and $\Delta M(q)$, $\Delta C(q, \dot{q})$ and $\Delta G(q)$ are the deviations between the reference model parameters and the actual model parameters.

Combining Eq. (11), Eq. (10) can be further formulated that

$$M_0(q)\ddot{q} + C_0(q, \dot{q})\dot{q} + G_0(q) = \tau + d \tag{12}$$

Where $d = \tau_d - \Delta M\dot{q} - \Delta C\dot{q} - \Delta G$ is a composite disturbance.

Then, Eq. (12) can be expressed by the following equation of state

$$\begin{cases} \dot{y}_1 = y_2 \\ \dot{y}_2 = F + B\tau + D \end{cases} \tag{13}$$

Where $F = -M_0^{-1}(C_0\dot{q} + G_0)$, $B = M_0^{-1}$, $D = M_0^{-1}d$.

Based on the physical properties of industrial robots, the system composite uncertainty term D in Eq. (12) contains internal parameter errors and external perturbations, but these uncertainties are bounded, i.e., $\|D\| \leq \eta$. If the acceleration signals are not included in the control inputs, then we can represent it using a function that contains only position and velocity measurements in the following form

$$\|D\| \leq \eta = \varphi_0 + \varphi_1 \|q\| + \varphi_2 \|\dot{q}\|^2 \tag{14}$$

Where φ_0, φ_1 and φ_2 are known non-negative constants, and η is the upper bound of the composite perturbation. The corresponding usage can be found in [25–29].

3. Control scheme design

This section presents an adaptive nonsingular fast TSMC (NFTSMC) algorithm for tracking control of a stiff manipulator. This algorithm exhibits rapid convergence and is free of singularities. Additionally, the algorithm's convergence time remains unaffected no matter what the initial state of the system is. The maximum extent of composite disturbances is often difficult to determine due to the intricate and unpredictable nature of practical work. Therefore, we add an adaptive algorithm to compensate on the basis of NFTSMC.

The tracking errors in position and velocity for the manipulator are as follows

$$e = q - q_d, \quad \dot{e} = \dot{q} - \dot{q}_d \tag{15}$$

To aid in the design of the control algorithm mentioned above, it has been separated into two components: TSM and joint control torque design.

Prior to the design of the TSM, inspired by the [20], we proposed the design of a new nonlinear continuous function $h(x)$.

$$h(x) = \begin{cases} \left(a|x|^{r_1-\frac{1}{r_2}} + a_3|x|^{r_3-\frac{1}{r_2}} + \beta\right)^{r_2} & |x| \geq \delta \\ \left(a_1|x|^{1-\frac{1}{r_2}} + a_2|x|^{2-\frac{1}{r_2}} + \beta\right)^{r_2} & |x| < \delta \end{cases} \tag{16}$$

Where each parameter is a normal number and satisfies $a > 0, \beta > 0, r_1 > 1, 1 < r_2 < 2, r_3 > 1, \quad 0 < \delta < 1, \quad a_1 = a\left(2 - r_1\right)\delta^{r_1-1} + a_3\left(2 - r_3\right)\delta^{r_3-1}, \quad a_2 = a\left(r_1 - 1\right)\delta^{r_1-2} + a_3\left(r_3 - 1\right)\delta^{r_3-2}$.

Based on the above nonlinear function $h(x)$, a nonsingular sliding mode surface (NFTSM) with fast response is designed

$$s = H(e)e + \mathrm{sig}^{r_2}(\dot{e}) \tag{17}$$

Where $H(e) = \mathrm{diag}\left(h_1\left(e_1\right), h_2\left(e_2\right), \cdots, h_i\left(e_i\right)\right)$.

For the above sliding surface, when the NFTSM $s = 0$, according to the sliding surface of Eq. (17), the trajectory of the manipulator transitions to the sliding stage from the arrival stage. Based on Eq. (17) and nonlinear function $h(x)$, the position convergence process of the sliding stage can be divided into two cases.

$$\dot{e}_i = \begin{cases} -\mathrm{asig}^{r_2}\left(e_i\right) - a_3\,\mathrm{sig}^{r_3}\left(e_i\right) - \beta\,\mathrm{sig}^{\frac{1}{r_2}}\left(e_i\right) & |e_i| \geq \delta \\ -a_1 e_i - a_2 e_i^2\,\mathrm{sign}\left(e_i\right) - \beta\,\mathrm{sig}^{\frac{1}{r_2}}\left(e_i\right) & |e_i| < \delta \end{cases} \tag{18}$$

Case 1: $|e_i| \geq \delta$. For this case, consider the selected Lyapunov function as

$$V_1 = \frac{1}{2}e_i^T e_i \tag{19}$$

Derivation of V_1, and substitute Eq. (18) into

$$\begin{aligned} \dot{V}_1 = e^T\dot{e} &= e^T\left(-a_{sig}g^{r_2}\left(e_i\right) - a_3\,\mathrm{sig}^{r_3}\left(e_i\right) - \beta\,\mathrm{sig}^{\frac{1}{r_2}}\left(e_i\right)\right) \\ &= -a\sum_{i=1}^{2}|e_i|^{r_2+1} - a_3\sum_{i=1}^{2}|e_i|^{r_3+1} - \beta\sum_{i=1}^{2}|e_i|^{\frac{1}{r_2}+1} \\ &= -a\sum_{i=1}^{2}\left(|e_i|^2\right)^{\frac{r_2+1}{2}} - a_3\sum_{i=1}^{2}\left(|e_i|^2\right)^{\frac{r_3+1}{2}} - \beta\sum_{i=1}^{2}\left(|e_i|^2\right)^{\frac{r_2+1}{2r_2}} \\ &\leq -a\sum_{i=1}^{2}\left(|e_i|^2\right)^{\frac{r_2+1}{2}} - \beta\sum_{i=1}^{2}\left(|e_i|^2\right)^{\frac{r_2+1}{2r_2}} \end{aligned} \tag{20}$$

From Lemma 3, Eq. (20) can be further simplified to

$$\dot{V}_1 \leq -2^{\frac{1-r_2}{2}}a\,\|e_i\|^{r_2+1} - \beta\|e\|^{\frac{1}{r_2}+1} \tag{21}$$

Substitute Eq. (19) into Eq. (21) to get

$$\dot{V}_1 \leq -2aV_1^{\frac{r_2+1}{2}} - \beta 2^{\frac{r_2+1}{2r_2}}V_1^{\frac{r_2+1}{2r_2}} \tag{22}$$

Then the convergence time t_1 can be obtained by Lemma 1.

$$t_1 \leq \frac{1}{a\left(r_2 - 1\right)} + \frac{2r_2}{\beta_1\left(r_2 - 1\right)} \tag{23}$$

Where $\beta_1 = 2^{\frac{r_2+1}{2r_2}}\beta$.

Case 2: $|e_i| < \delta$. For this case, the Lyapunov function is proposed as

$$V_2 = \frac{1}{2}e_i^T e_i \tag{24}$$

Derivation of V_2, and substitute Eq. (18) into

$$\begin{aligned} \dot{V}_2 &= e^T\left(-a_1 e_i - a_2 e_i^2\,\mathrm{sign}\left(e_i\right) - \beta\,\mathrm{sig}^{\frac{1}{r_2}}\left(e_i\right)\right) \\ &= -a_1\sum_{i=1}^{2}|e_i|^2 - a_2\sum_{i=1}^{2}|e_i|^3 - \beta\sum_{i=1}^{2}|e_i|^{\frac{1}{r_2}+1} \\ &= -2a_1V_2 - a_2 2^{\frac{3}{2}}V_2^{\frac{3}{2}} - \beta 2^{\frac{r_2+1}{2r_2}}V_2^{\frac{r_2+1}{2r_2}} \\ &= -\sigma_1 V_2 - \sigma_2 V_2^{\frac{3}{2}} - \sigma_3 V_2^{\beta_2} \end{aligned} \tag{25}$$

Where $\sigma_1 = 2a_1, \quad \sigma_2 = 2^{\frac{3}{2}}a_2, \quad \sigma_3 = 2^{\frac{r_2+1}{r_2}}\beta, \quad \beta_2 = \frac{1}{2}\left(\frac{1}{r_2} + 1\right)$.

Then the convergence time t_2 can be obtained by Lemma 2.

$$t_2 \leq \frac{2}{\sigma_1}\ln\left(1 + \frac{\sigma_1}{\sigma_2}\right) + \frac{2r_2}{\sigma_1\left(r_2 - 1\right)}\ln\left(1 + \frac{\sigma_1}{\sigma_3}\right) \tag{26}$$

From the above analysis, it can be seen that the manipulator system will make the trajectory error tend to zero in a fixed time T_1.

$$T_1 \leq t_1 + t_2 \tag{27}$$

Remark 1. Eq. (17) of the SM surface is inspired by the work presented in [20]. Differing from [20], we design a novel nonlinear function $h(x)$ in Eq. (17) to enhance the convergence speed of the error. By adjusting the parameter gain, an upper bound on its convergence time can be calculated.

3.1. NFTSMC design

Define a new nonlinear function as

$$\rho(x) = \begin{cases} \sin\left(\frac{\pi}{2}\frac{x}{\mu}\right) & x < \mu \\ 1 & x \geq \mu \end{cases} \tag{28}$$

Where $\rho(x)$ is a non-negative function, and $\mu > 0$ in the function is a parameter to be designed.

According to the selected NFTSMC, the following controller is designed

$$\tau = \tau_1 + \tau_2 + \tau_3 \tag{29}$$

$$\begin{aligned} \tau_1 &= M\ddot{q}_d + C\dot{q} + G \\ &- \frac{1}{r_2} M\left\{\tilde{H}\left(e_i\right) + H\left(e_i\right)\right\} \operatorname{sig}^{2-r_2}(\dot{e}) \end{aligned} \tag{30}$$

$$\begin{aligned} \tau_2 = &-\frac{1}{r_2}\operatorname{Mdiag}\left\{\rho\left(|e_i|^{r_2-1}\right)\right\} \\ &\operatorname{diag}\left\{\left(|e_i|^{1-r_2}\right)\right\}\left\{\lambda_1 \operatorname{sig}^{r_4}(s) + \lambda_2 \operatorname{sig}^{r_5}(s)\right\} \end{aligned} \tag{31}$$

$$\tau_3 = -M\frac{\theta s}{\|\theta s\|}\left(\varphi_0 + \varphi_1\|q\| + \varphi_2\|\dot{q}\|^2\right) \tag{32}$$

Where λ_1 and λ_2 are integral constants, $0 < r_4 < 1, r_5 > 1, \theta = \operatorname{diag}\left(\theta_1, \theta_2, \cdots, \theta_i\right)$, $\theta_i = r_2\dot{e}_i^{r_2-1} \cdot \tilde{H}(e) = \operatorname{diag}\left(\tilde{h}_1\left(e_1\right), \tilde{h}_2\left(e_2\right), \cdots, \tilde{h}_i\left(e_i\right)\right).\tilde{h}_i\left(e_i\right)$ is denoted by

$$\tilde{h}_i\left(e_i\right) = \begin{cases} r_2\left(a|e_i|^{r_1-\frac{1}{r_2}} + a_3|e_i|^{r_3-\frac{1}{r_2}} + \beta\right)^{r_2-1} \\ \left(a\left(r_1-\frac{1}{r_2}\right)|e_i|^{r_1-\frac{1}{r_2}} + a\left(r_3-\frac{1}{r_2}\right)|e_i|^{r_3-\frac{1}{r_2}}\right) \\ |e_i| \geq \delta \\ r_2\left(a_1|e_i|^{1-\frac{1}{r_2}} + a_2|e_i|^{2-\frac{1}{r_2}} + \beta\right)^{r_2-1} \\ \left\{a_1\left(1-\frac{1}{r_2}\right)|e_i|^{1-\frac{1}{r_2}} + a_2\left(2-\frac{1}{r_2}\right)|e_i|^{2-\frac{1}{r_2}}\right\} \\ |e_i| < \delta \end{cases} \tag{33}$$

For the control schemes Eq. (29) - Eq. (32) in the equation, the tracking error converges in a fixed time, which is denoted as T. This time period can be further divided into two different stages: the arrival time, recorded as T_1, and the sliding time, recorded as T_2. The arrival time indicates the time that the system takes to reach the surface after a period of time from the initial state. The sliding time signifies the time when the tracking error gradually approaches the small area near the origin on the sliding surface. T_2 denotes as

$$T_2 \leq \frac{1}{\omega_1}\frac{2}{r_4-1} + \frac{1}{\omega_2}\frac{2}{r_5-1} \tag{34}$$

Proof. Select the following Lyapunov function

$$V_3 = \frac{1}{2}s^2 \tag{35}$$

Derivative of V_3

$$\begin{aligned} \dot{V}_3 =& s^T\dot{s} \\ =& -s^T\left\{\operatorname{diag}\left\{\rho\left(|e_i|^{r_2-1}\right)\right\}\right\}\left\{\lambda_1 \operatorname{sig}^{r_4}(s) + \lambda_2 \operatorname{sig}^{r_5}(s)\right\} \\ &- \|\theta s\|\left(\varphi_0 + \varphi_1\|q\| + \varphi_2\|\dot{q}\|^2\right) + s^T\theta D \\ \leq& -s^T\left\{\operatorname{diag}\left\{\rho\left(|e_i|^{r_2-1}\right)\right\}\right\}\left\{\lambda_1 \operatorname{sig}^{r_4}(s) + \lambda_2 \operatorname{sig}^{r_5}(s)\right\} \\ &- \|\theta s\|\left(\varphi_0 + \varphi_1\|q\| + \varphi_2\|\dot{q}\|^2\right) + \left\|s^T\theta\right\|\|D\| \end{aligned} \tag{36}$$

In light of Eq. (14), the expression for $\dot{V}_3$ could be written as follows

$$\begin{aligned} \dot{V}_3 &\leq -s^T\left\{\operatorname{diag}\left\{\rho\left(|e_i|^{r_2-1}\right)\right\}\right\}\left\{\lambda_1 \operatorname{sig}^{r_4}(s) + \lambda_2 \operatorname{sig}^{r_5}(s)\right\} \\ &= -\lambda_1\rho\left(|e_i|^{r_2-1}\right)|s_i|^{r_4+1} - \lambda_2\rho\left(|e_i|^{r_2-1}\right)|s_i|^{r_3+1} \end{aligned} \tag{37}$$

According to Lemma 2 and Eq. (35), Eq. (37) is transformed into

$$\dot{V}_3 \leq -\omega_1 V_3^{\frac{1+r_4}{2}} - \omega_2 V_3^{\frac{1+r_5}{2}} \tag{38}$$

Where $\omega_1 = \min\left\{\lambda_1 2^{\frac{1+r_4}{2}}\rho\left(|\dot{e}_i|^{r_2-1}\right)\right\}, \omega_2 = \min\left\{\lambda_2 2^{\frac{1+r_5}{2}}\rho\left(|\dot{e}_i|^{r_2-1}\right)\right\}$.

Since $0 < r_4 < 1$ and $r_5 > 1$ are normal numbers, the trajectory motion will eventually reach a stable state within a predetermined time. This fixed time T_2 can be verified by Eq. (34).

3.2. ANFTSMC design

However, the control strategy presented in Section 2.1 is rooted in our understanding of the uncertainties in system coupling. Yet, this control scheme often struggles to meet the standards of industrial robots, making it arduous to ensure the implementation of control law τ. The upper bound of its perturbation is dealt with by introducing adaptive. Eq. (29) and Eq. (32) are denoted by

$$\tau = \tau_1 + \tau_2 + \tau_3^* \tag{39}$$

$$\tau_3^* = -M\frac{\theta s}{\|\theta s\|}\left(\hat{\varphi}_0 + \hat{\varphi}_1\|q\| + \hat{\varphi}_2\|\dot{q}\|^2\right) \tag{40}$$

Where $\dot{\hat{\varphi}}_i$ is the approximated value of φ_i, and its parameter adaptive update equation $\dot{i}$

$$\dot{\hat{\varphi}}_0 = \|\theta s\|, \quad \dot{\hat{\varphi}}_1 = \|\theta s\|\|q\|, \quad \dot{\hat{\varphi}}_2 = \|\theta s\|\|\dot{q}\|^2 \tag{41}$$

Proof. Select the following Lyapunov function

$$V_4 = \frac{1}{2}s^2 + \sum_{i=0}^{2}\frac{1}{2}\left(\hat{\varphi}_i - \varphi_i\right)^2 \tag{42}$$

Derivation of V_4

$$\dot{V}_4 = s\dot{S} + \sum_{i=0}^{2}\left(\hat{\varphi}_i - \varphi_i\right)\dot{\hat{\varphi}}_i \tag{43}$$

Consider Eqs. (13) and (14), the above equations can be formulated as follows

$$\dot{V}_4 = -s^T \left\{ \frac{dH(e)}{dt} e + H(e)\dot{e} + r_2 \operatorname{diag}\left\{ |\dot{e}|^{r_2-1} \right\} \right. \\ \left. (F + B\tau + D - \ddot{q}_d) \right\} + \sum_{i=0}^{2} (\hat{\varphi}_i - \varphi_i)\, \dot{\hat{\varphi}}_i \tag{44}$$

Combining Eqs. (39) and (41), the specific time derivative of V_4 is obtained.

$$\begin{aligned} \dot{V}_4 &= -s^T \operatorname{diag}\left\{ \rho\left(|\dot{e}|^{r_2-1} \right) \right\} \left\{ \lambda_1 \operatorname{sig}^{r_4}(s) + \lambda_2 sig^{r_5}(s) \right\} \\ &- s^T \left\{ r_2 \operatorname{diag}\left(|\dot{e}|^{r^2-1} \right) \right\} \left\{ \frac{\theta s}{\|\theta s\|} \left(\hat{\varphi}_0 + \hat{\varphi}_1 \|q\| + \hat{\varphi}_2 \|\dot{q}\|^2 \right) - D \right\} \\ &+ (\hat{\varphi}_0 - \varphi_0) \|\theta s\| + (\hat{\varphi}_1 - \varphi_1) \|\theta s\| \|q\| + (\hat{\varphi}_2 - \varphi_2) \|\theta s\| \|\dot{q}\|^2 \\ &\le -s^T \operatorname{diag}\left\{ \rho\left(|\dot{e}|^{r_2-1} \right) \right\} \left\{ \lambda_1 \operatorname{sig}^{r_4}(s) + \lambda_2 \operatorname{sig}^{r_5}(s) \right\} \\ &+ \|\theta s\| \left\{ \|D\| - \left(\varphi_0 + \varphi_1 \|q\| + \varphi_2 \|\dot{q}\|^2 \right) \right\} \end{aligned} \tag{45}$$

Because of $\|D\| - \left(\varphi_0 + \varphi_1\|q\| + \varphi_2\|\dot{q}\|^2\right) \le 0$, then Eq. (45) can be expressed as

$$\dot{V}_4 \le -\lambda_1 \rho\left(|e_i|^{r_2-1} \right) |s_i|^{r_4+1} - \lambda_2 \rho\left(|e_i|^{r_2-1} \right) |s_i|^{r_5+1} \tag{46}$$

By comparing Eq. (46) to Eq. (38), it is evident that both schemes have identical setting times. This implies that the expected tracking can be achieved and proven to be completed.

Remark 2. It is important to note that in practice, the discontinuity term τ_3^* in Eq. (40) may lead to the appearance of jitter vibration. Usually, a boundary layer approach can be used for diminishing the jitter vibration of the system, i.e., Eq. (40) is modified to be

$$\tau_3^* = -\frac{M\theta s}{\|\theta s\| + 0.0005} \left(\hat{\varphi}_0 + \hat{\varphi}_1 \|q\| + \hat{\varphi}_2 \|\dot{q}\|^2 \right) \tag{47}$$

4. Results from experiments and corresponding analysis

To determine the efficacy and superiority of the ANFSMC suggested in Section 3.2, it was implemented in the control system of manipulator. For rigid two-joint manipulator systems, there are

$$\begin{bmatrix} M_{11}(q) & M_{12}(q) \\ M_{21}(q) & M_{22}(q) \end{bmatrix} \begin{bmatrix} \ddot{q}_1 \\ \ddot{q}_2 \end{bmatrix} + \begin{bmatrix} C_{11}(q,\dot{q}) & C_{12}(q,\dot{q}) \\ C_{21}(q,\dot{q}) & C_{22}(q,\dot{q}) \end{bmatrix} \begin{bmatrix} \dot{q}_1 \\ \dot{q}_2 \end{bmatrix} + \begin{bmatrix} G_1(q) \\ G_2(q) \end{bmatrix} = \begin{bmatrix} \tau_1 \\ \tau_2 \end{bmatrix} \tag{48}$$

Where $M_{11}(q) = (m_1 + m_2) l_1^2 + m_2 l_2^2 + 2m_2 l_1 l_2 \cos(q_2) + J_1$, $M_{12}(q) = m_2 l_2^2 + m_2 l_1 l_2 \cos(q_2)$, $M_{21}(q) = M_{21}(q)$, $M_{22}(q) = m_2 l_2^2 + J_2$, $C_{11}(q,\dot{q}) = -2m_2 l_1 l_2 \sin(q_2)\dot{q}_2$ $C_{12}(q,\dot{q}) = -(1/2)C_{11}(q,\dot{q})$, $C_{21}(q,\dot{q}) = m_2 l_1 l_2 \sin(q_2)\dot{q}_1$, $C_{22}(q,\dot{q}) = 0$, $p_1 = (m_1 + m_2) g l_1 \cos(q_1)$, $p_2 = m_2 g l_2 \cos(q_1 + q_2)$, $G_1(q) = p_1 + p_2$, $G_2(q) = p_2$

The relevant characteristics of the two-joint manipulator system are as follows : $l_1 = 1$ m, $l_2 = 0.8$ m, $m_1 = 0.5$ kg, $m_2 = 1.5$ kg, $J_1 = J_2 = 5$ kg $\cdot$ m^2. In the formula, l_i is the length of the joint i, m_i is the mass of the joint, J_i is the inertia of the joint, $i = 1, 2$. The gravitational acceleration is $g = 9.8$ m/s^2. The reference values of m_1, m_2, J_1 and J_2 are 0.6 kg, 1.8 kg, 6 kg $\cdot$ m^2 and 6 kg $\cdot$ m^2, respectively.

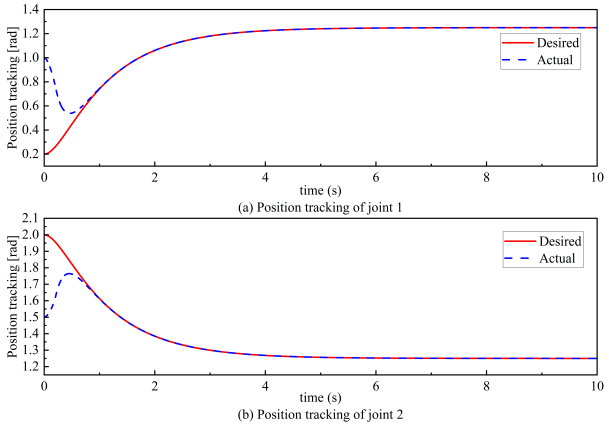

Fig. 1. Tracking performance of position.

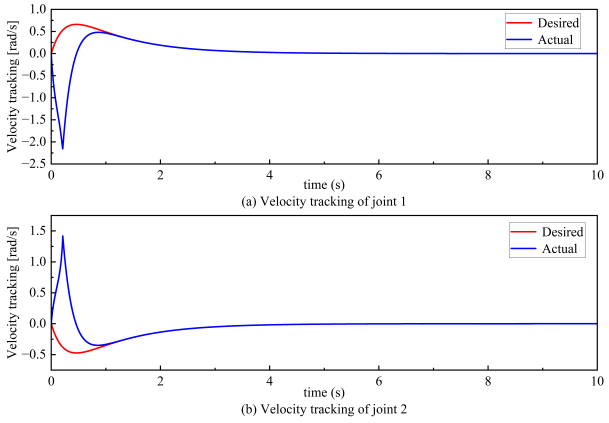

Fig. 2. Tracking performance of speed.

External interference is

$$\tau_d = \begin{bmatrix} \tau_{d1} \\ \tau_{d2} \end{bmatrix} = \begin{bmatrix} 0.5\sin(200\pi t) + 2\sin(t) \\ 0.5\sin(200\pi t) + \cos(2t) \end{bmatrix} \tag{49}$$

The expected trajectory $q = \begin{bmatrix} q_{d1} & q_{d2} \end{bmatrix}^T$ is

$$q_d = \begin{bmatrix} q_{d1} \\ q_{d2} \end{bmatrix} = \begin{bmatrix} -1.4e^{-t} + 0.35e^{-4t} + 1.25 \\ e^{-t} - 0.25e^{-4t} + 1.25 \end{bmatrix} \tag{50}$$

The system's starting position and velocity are designated as $q(0) = \begin{bmatrix} 1 & 1.5 \end{bmatrix}^T$ and $\dot{q}(0) = \begin{bmatrix} 0 & 0 \end{bmatrix}^T$. Table 1 provides an overview of the control parameter values proposed in Section 3.2.

4.1. Performance verification of ANFTSMC

With coupling uncertainty, the control performance of the manipulator is demonstrated in Figs. 1 to Figs. 5. They respectively display the tracking performance of the position and velocity, as well as its corresponding error convergence ability, joint torque, and estimated lumped disturbance parameters. Figs.1 and Figs. 2 illustrate that the ANFTSMC algorithm presented in this paper successfully guarantees convergence of the manipulator's joint position to the desired trajectory within a predetermined time range, even when uncertain coupling with unknown upper bounds is present. In addition, Fig. 3 shows the convergence of the system error to zero over time. By observing Fig. 4, it is clear that the control torque resulting from the system is continuous, uninterrupted and does not change instantaneously and drastically during the control process. The results of Fig. 5 show that the lumped disturbance parameters of the system are finally stable after the estimation of the adaptive law. These simulation experiments indicate that the designed ANFTSMC demonstrates remarkable tracking accuracy, rapid response capability, no singularity, and excellent robust performance.

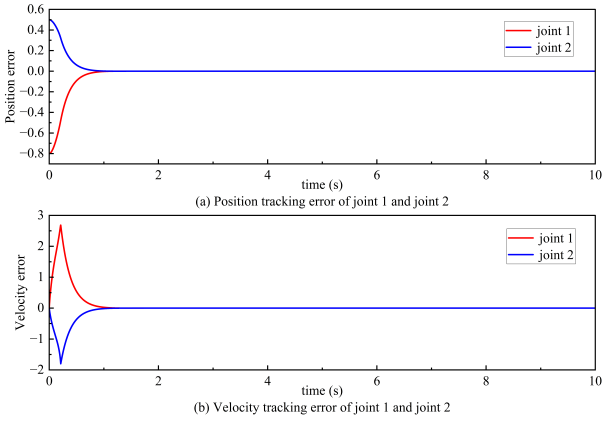

Fig. 3. Tracking errors of position and velocity.

4.2. Evaluation of ANFTSMC Performance

Compare and analyze ANFTSMC [16], FNTSMC [17] and SFSMC [21] to ascertain the excellent control performance of the implemented ANFTSMC technology. To ensure the credibility and realism of the simulation results, identical initial conditions are adopted for all simulations.

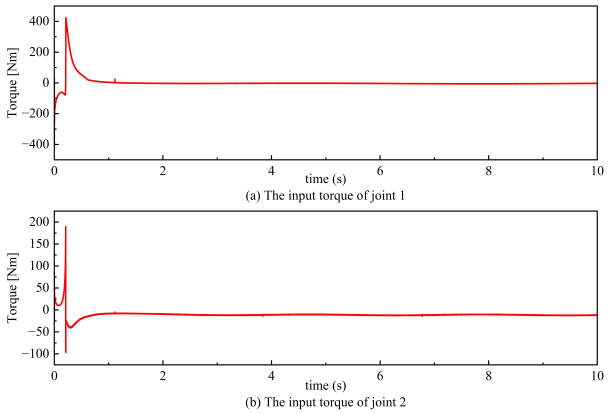

Fig. 4. Control torque of joint 1 and joint 2.

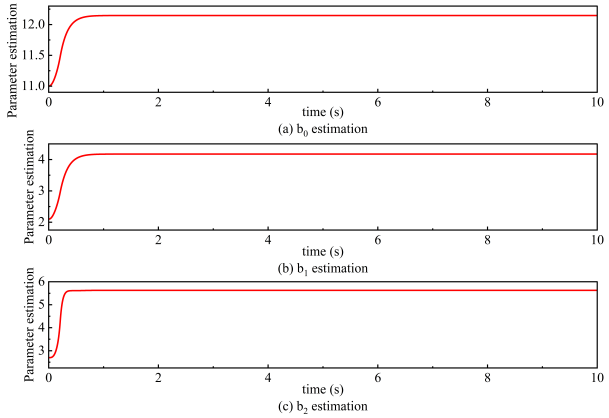

Fig. 5. Adaptive parameter estimation.

The control scheme and adaptive law of ANFTSMC [16] can be described as

$$
\begin{aligned}
&s = x_1 + k_1 |x_1|^{\alpha} \operatorname{sign}(x_1) + k_2 |x_2|^{\beta} \operatorname{sign}(x_2) \\
&\dot{\hat{\omega}}_1 = \rho_0 \|s\| \, \|x_2\|^{\beta-1} \quad \dot{\hat{\omega}}_2 = \rho_1 \|s\| \, \|x_2\|^{\beta-1} \, \|q\| \\
&\dot{\hat{\omega}}_3 = \rho_2 \|s\| \, \|x_2\|^{\beta-1} \, \|\dot{q}\|^2 \\
&\tau = \tau_{eq} + \tau_{csw} \\
&\tau_{eq} = M_0 \ddot{q}_d + C_0 \dot{q} + G_0 \\
&- \frac{M_0}{\beta k_2} |x_2|^{2-\beta} \left(1 + \alpha k_1 |x_1|^{\alpha-1}\right) \operatorname{sign}(x_2) \\
&\tau_{csw} = -M_0 \left[ks + \left(\hat{\omega}_1 + \hat{\omega}_1 \|q\| + \hat{\omega}_3 \|\dot{q}\|^2 + \eta\right) \operatorname{sign}(s) \right]
\end{aligned} \tag{51}
$$

Where $\alpha, \beta, \eta, k_1, k_2, \rho_0, \rho_1$, and ρ_2 are already known normal number, and $\hat{\omega}_1$, $\hat{\omega}_2$, and $\hat{\omega}_3$ are used to provide an estimate of the maximum limit on the uncertainty term of the system.

Table 1. Control parameters.

Parameter	Value	Parameter	Value	Parameter	Value
a	1.8	r_1	1.2	λ_1	0.6
a_3	1.55	r_2	1.25	λ_2	0.6
β	2.4	r_3	1.25	$\hat{\varphi}_0(0)$	11
δ	0.001	r_4	18/24	$\hat{\varphi}_1(0)$	2.1
μ	0.1	r_5	1.6	$\hat{\varphi}_2(0)$	2.7

The FNTSMC [17] can be described as

$$\begin{aligned} s &= x_1 + \operatorname{sig}^{\gamma_1}(x_1) + \operatorname{sig}^{\gamma_2}(x_2) \\ \tau &= -M_0 \left[K_2 s + (\xi + s)\frac{s}{\|s\|} + F_2 + \gamma_2^{-1} \right. \\ &\quad \left. \left(I_2 + \gamma_1 D^{\gamma_1 - 1}(x_1)\right) \operatorname{sig}^{2-\gamma_2}(x_2) \right] \\ \xi &= \left\| M_0^{-1} \right\| \left(b_0 + b_1 \|q\| + b_2 \|\dot{q}\|^2 \right) \\ F_2 &= -M_0^{-1}(C_0 \dot{q} + G_0) - \ddot{q}_d \end{aligned} \tag{52}$$

Where K_1, K_2, γ_1, and γ_2 are known positive number. Furthermore, in this scheme, b_0, b_1 and b_2 are also known normals, indicating that the maximum limit of the uncertainty term is known in the system.

The SFSMC [21] can be described as

$$\begin{aligned} s &= x_2 + C_1 F(x_1) + C_2 \operatorname{sig}^{\beta}(x_1) \\ \tau &= \tau_0 + \tau_1 + \tau_2 \\ \tau_0 &= M_0 \ddot{q}_d + C_0 \dot{q} + G_0 - C_1 M_0 A(x_1) x_2 \\ &\quad - C_2 M_0 B^{\beta - 1}(x_1) x_2 \\ \tau_1 &= -K_1 \operatorname{sig}^{\gamma_1}(s) - K_2 \operatorname{sig}^{\gamma_2}(s) \\ \tau_2 &= -b(s)\frac{1}{1-\sigma}\left(b_0 + b_1 \|\dot{q}\|^2 + \sigma \|\tau_1 + \tau_0\| \right) \\ b(s) &= \begin{cases} \frac{s}{\|s\|} & \|s\| \neq 0 \\ 0 & \|s\| = 0 \end{cases} \\ F(x_1) &= \left[\, f(x_{11}), f(x_{12}), \cdots, f(x_{1n}) \, \right]^T \\ f(x_1) &= \begin{cases} K_a \operatorname{sig}^{r}(x) + K_b \delta^{|x|} x & |x| < \delta \\ \operatorname{sig}^{\alpha}(x) & |x| \geq \delta \end{cases} \end{aligned} \tag{53}$$

Where $\alpha, \beta, \gamma_1, \gamma_2, a, \delta$ and r are known positive number and C_1 and C_2 are known second order positive definite diagonal matrices. In addition, the uncertainty terms in the scheme are also known, so that $b_i (i = 0, 1)$ is known constants.

Table 2 lists the corresponding parameters for the above schemes. Fig. 6 compares the convergence speed of the three schemes in joint position tracking. The convergence performance of the scheme introduced in this investigation is better than the other two. Fig. 7 clearly compares the corresponding torques under different controllers. From the figure, we can see that the scheme exhibits smoother input characteristics against external disturbances.

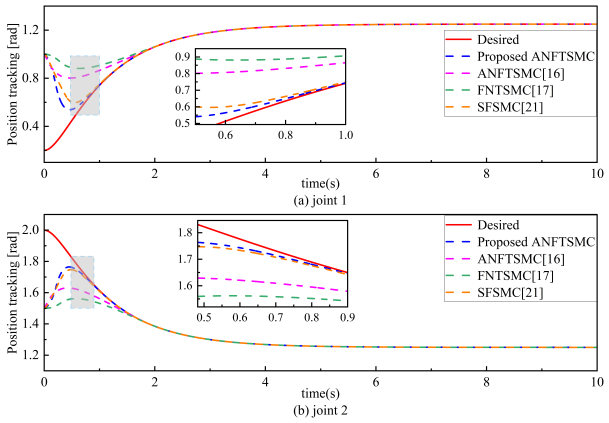

Fig. 6. Comparison diagram of joint position convergence.

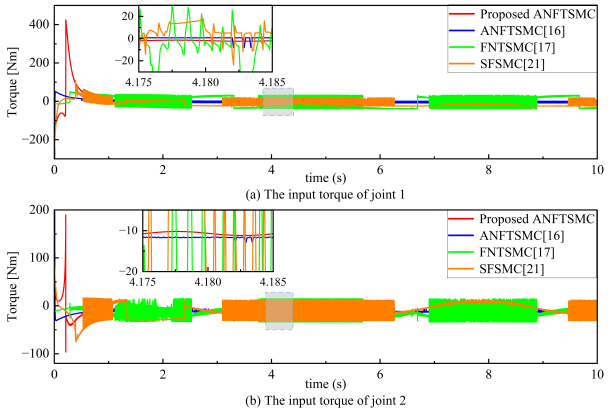

Fig. 7. Comparison of input torque of two joints.

In order to more rigorously demonstrate the effectiveness of our proposed methodology, we will introduce integral absolute error (IAE) and integral of the square value (ISV) to measure the controller scheme. By combining ISV and IAE, a more comprehensive convergence analysis can be obtained. In addition, we added data on the adjustment time of the robotic arm to measure the rapid responsiveness of the system.

$$IAE = \int_0^t |x - x_d| \, dt \tag{54}$$

and

$$ISV = \int_0^t \tau^2 dt \tag{55}$$

Upon comparison of the controller schemes examined,

Table 2. Parameters of the comparison scheme.

Control Scheme	Parameter Values
ANFTSMC[16]	$\alpha = 0.2, \beta = 5/3, k_1 = k_2 = 1, \eta = 250, \rho_0 = \rho_1 = \rho_2 = 0.01,$ $k = 250, \hat{\omega}_1(0) = \hat{\omega}_2(0) = \hat{\omega}_3(0) = 0$
FNTSMC[17]	$\gamma_1 = 2, \gamma_2 = 5/3, K_1 = 1, K_2 = 2 \quad b_0 = 12, b_1 = 2.2, b_2 = 2.8$
SFSMC[21]	$\alpha = 0.7, \beta = 1.9, \gamma_1 = 2.5, \gamma_2 = 0.5, C_1 = C_2 = 3I_2, K_1 = K_2 = 5I_2,$ $r = 1.7, \delta = 0.3, b_0(0) = 12, b_1(0) = 2.2$

Table 3. Quantitative analysis.

Controller	IAE		ISV		Adjustment time	
	Joint 1	Joint 2	Joint 1	Joint 2	Joint 1	Joint 2
Proposed ANFTSMC	0.2262	0.1470	0.9257	0.2091	1.113	1.042
ANFTSMC[16]	0.4222	0.2317	1.8680	0.3547	1.895	1.593
FNTSMC[17]	0.5221	0.3020	0.8396	0.2865	2.025	1.744
SFSMC[21]	0.2702	0.1563	0.3657	0.4579	1.362	1.237

it is evident from the simulation comparison illustrated in Fig. 6 and Table 3 that the control performance of the joints in the ANFTSMC [16] and FNTSMC [17] are significantly slower than that of the other two control schemes. For joints 1 and 2, the controllers designed in this paper save 41.27% and 34.59% convergence time compared to ANFTSMC [16] and 45.04% and 40.25% compared to FNTSMC [17], respectively. Additionally, based on Table 3, the IAE value of the ANFTSMC scheme proposed in this study is lower in comparison to the SFSMC scheme [21]. The calculated IAE for the design solution were reduced by 16.28% and 5.95%, respectively. In Fig. 7, the ANFTSMC [16] scheme requires a large initial control input and there is chattering in the subsequent control. Although the ISV of joint one for FNTSMC [17] and SFSMC [21] are smaller in Table 3, their moment inputs are observed to fluctuate more in Fig. 7, suggesting that there is a severe jitter vibration in the manipulator. Compared to traditional methods, the proposed ANFSMC scheme offers a more consistent and streamlined control input, effectively eradicating any chattering phenomenon present in the robotic arm's control torque.

5. Conclusions

A novel control strategy in this paper is proposed to address the fixed-time trajectory tracking challenges of manipulators under internal parameter errors and external perturbations. The recommended method aims to promise that the system's error converges over a fixed duration and can overcome the need for prior knowledge of the disturbances and uncertainties while mitigating the singularity of sliding mode. The results of the simulation experiments indicated that the suggested method is more rapid in terms of convergence speed and the control torque is continuous, stable and free of chattering compared to the existing control schemes. This ensures smooth movement of the mechanical system during control adjustments and reduces wear and tear on the mechanical system, which is more conducive to use in actual industry. Finally, through an in-depth discussion of practical applications and broader implications, we hope that this program will play a role in improving work efficiency, enhancing the safety of robot operation, and accuracy. In the ensuing stages, we intend to substantiate the validity of the control strategy envisaged in this document in actual projects and refine it continuously.

Acknowledgments

This work is funded by the Natural Science Foundation of Gansu Province (Grant No. 20JR5RA419), Gansu Province Higher Education Innovation Fund Project (Grant No. 2022A-045), National Natural Science Foundation of China" (Grant No. 62341310) and Lanzhou Jiaotong University-Tianjin University Innovation Fund Project (Grant No. 2019053).

References

[1] M. Van, X. P. Do, and M. Mavrovouniotis, (2020) *"Self-tuning fuzzy PID-nonsingular fast terminal sliding mode control for robust fault tolerant control of robot manipulators"* **ISA Transactions *96***: 60–68. DOI: 10.1016/j.isatra.2019.06.017.

[2] B. K. Yoo and W. C. Ham, (2000) *"Adaptive control of robot manipulator using fuzzy compensator"* **IEEE Transactions on Fuzzy Systems** *8*(2): 186–199. DOI: 10.1109/91.842152.

[3] H. Liu and T. Zhang, (2013) *"Neural network-based robust finite-time control for robotic manipulators considering actuator dynamics"* **Robotics and Computer-Integrated Manufacturing *29***(2): 301–308. DOI: 10.1016/j.rcim.2012.09.002.

[4] Z. Li, W. He, Z. Tao, and C. Liu, (2013) *"Deterministic Learning Control of a Robotic System Via Neural Networks"* **IFAC Proceedings Volumes *46***(20): 695–700. DOI: 10.3182/20130902-3-CN-3020.00172.

[5] X. Liang, H. Wang, and Y. Zhang, (2022) *"Adaptive nonsingular terminal sliding mode control for rehabilitation robots"* **Computers and Electrical Engineering *99***: 107718. DOI: 10.1016/J.COMPELECENG.2022.107718.

[6] T. Mai and H. Tran, (2023) *"An adaptive robust backstepping improved control scheme for mobile manipulators robot"* **ISA Transactions *137***: 446–456. DOI: 10.1016/J.ISATRA.2023.01.005.

[7] M. Van, M. Mavrovouniotis, and S. S. Ge, (2018) *"An adaptive backstepping nonsingular fast terminal sliding mode control for robust fault tolerant control of robot manipulators"* **IEEE Transactions on Systems, Man, and Cybernetics: Systems *49***(7): 1448–1458. DOI: 10.1109/TSMC.2017.2782246.

[8] N. Adhikary and C. Mahanta, (2018) *"Sliding mode control of position commanded robot manipulators"* **Control Engineering Practice *81***: 183–198. DOI: 10.1016/j.conengprac.2018.09.011.

[9] J. Su, J. Yang, and S. Li, (2014) *"Continuous finite-time anti-disturbance control for a class of uncertain nonlinear systems"* **Transactions of the Institute of Measurement and Control *36***(3): 300–311. DOI: 10.1177/0142331213499182.

[10] H. Rabiee, M. Ataei, and M. Ekramian, (2019) *"Continuous nonsingular terminal sliding mode control based on adaptive sliding mode disturbance observer for uncertain nonlinear systems"* **Automatica *109***: 108515. DOI: 10.1016/j.automatica.2019.108515.

[11] A. Vahidi-Moghaddam, A. Rajaei, and M. Ayati, (2019) *"Disturbance-observer-based fuzzy terminal sliding mode control for MIMO uncertain nonlinear systems"* **Applied Mathematical Modelling *70***: 109–127. DOI: 10.1016/j.apm.2019.01.010.

[12] Z. Anjum, Y. Guo, and W. Yao, (2021) *"Fault tolerant control for robotic manipulator using fractional-order backstepping fast terminal sliding mode control"* **Transactions of the Institute of Measurement and Control *43***(14): 3244–3254. DOI: 10.1177/01423312211022449.

[13] B. MOUDOUD, H. AISSAOUI, and M. DIANY. "Robust Trajectory Tracking with Adaptive Non-singular Fast TSM Control of a Robot Manipulator". In: IEEE. 2022, 1880–1885. DOI: 10.1109/SSD54932.2022.9955926.

[14] J. Geng, Y. Sheng, and X. Liu, (2014) *"Time-varying nonsingular terminal sliding mode control for robot manipulators"* **Transactions of the Institute of Measurement and Control *36***(5): 604–617. DOI: 10.1177/0142331213512367.

[15] Y.-J. Ma, H. Zhao, and T. Li, (2022) *"Robust adaptive dual layer sliding mode controller: Methodology and application of uncertain robot manipulator"* **Transactions of the Institute of Measurement and Control *44***(4): 848–860. DOI: 10.1177/01423312211025330.

[16] M. Boukattaya, N. Mezghani, and T. Damak, (2018) *"Adaptive nonsingular fast terminal sliding-mode control for the tracking problem of uncertain dynamical systems"* **ISA Transactions *77***: 1–19. DOI: 10.1016/j.isatra.2018.04.007.

[17] L. Yang and J. Yang, (2011) *"Nonsingular fast terminal sliding-mode control for nonlinear dynamical systems"* **International Journal of Robust and Nonlinear Control *21***(16): 1865–1879. DOI: 10.1002/rnc.1666.

[18] Y. Feng, X. Yu, and Z. Man, (2002) *"Non-singular terminal sliding mode control of rigid manipulators"* **Automatica *38***(12): 2159–2167. DOI: 10.1016/S0005-1098(02)00147-4.

[19] S. Mobayen, F. Tchier, and L. Ragoub, (2017) *"Design of an adaptive tracker for n-link rigid robotic manipulators based on super-twisting global nonlinear sliding mode control"* **International Journal of Systems Science *48***(9): 1990–2002. DOI: 10.1080/00207721.2017.1299812.

[20] J. Zhang, S. Yu, D. Wu, and Y. Yan, (2020) *"Nonsingular fixed-time terminal sliding mode trajectory tracking control for marine surface vessels with anti-disturbances"* **Ocean Engineering *217***: 108158. DOI: 10.1016/j.oceaneng.2020.108158.

[21] L. Zhang, Y. Wang, Y. Hou, and H. Li, (2019) *"Fixed-time sliding mode control for uncertain robot manipulators"* **IEEE Access *7***: 149750–149763. DOI: 10.1109/ACCESS.2019.2946866.

[22] Y. Wang, S. Li, D. Wang, F. Ju, B. Chen, and H. Wu, (2020) *"Adaptive time-delay control for cable-driven manipulators with enhanced nonsingular fast terminal sliding mode"* **IEEE Transactions on Industrial Electronics *68***(3): 2356–2367. DOI: 10.1109/tie.2020.2975473.

[23] Y. Wang, K. Zhu, B. Chen, and M. Jin, (2020) *"Model-free continuous nonsingular fast terminal sliding mode control for cable-driven manipulators"* **ISA Transactions** ***98***: 483–495. DOI: 10.1016/j.isatra.2019.08.046.

[24] Y. Hu, H. Yan, H. Zhang, M. Wang, and L. Zeng, (2022) *"Robust adaptive fixed-time sliding-mode control for uncertain robotic systems with input saturation"* **IEEE Transactions on Cybernetics** ***53***(4): 2636–2646. DOI: 10.1109/TCYB.2022.3164739.

[25] X. Zhang and R. Shi, (2022) *"Novel fast fixed-time sliding mode trajectory tracking control for manipulator"* **Chaos, Solitons & Fractals** ***162***: 112469. DOI: 10.1016/J.CHAOS.2022.112469.

[26] X. Zhang, R. Shi, Z. Zhu, and Y. Quan, (2023) *"Adaptive nonsingular fixed-time sliding mode control for manipulator systems' trajectory tracking"* **Complex & Intelligent Systems** ***9***(2): 1605–1616. DOI: 10.1007/S40747-022-00864-W.

[27] M. B. R. Neila and D. Tarak, (2011) *"Adaptive terminal sliding mode control for rigid robotic manipulators"* **International Journal of Automation and Computing** ***8***(2): 215–220. DOI: 10.1007/s11633-011-0576-2.

[28] S. Mondal and C. Mahanta, (2014) *"Adaptive second order terminal sliding mode controller for robotic manipulators"* **Journal of the Franklin Institute** ***351***(4): 2356–2377. DOI: 10.1016/j.jfranklin.2013.08.027.

[29] S. Yi and J. Zhai, (2019) *"Adaptive second-order fast nonsingular terminal sliding mode control for robotic manipulators"* **ISA Transactions** ***90***: 41–51. DOI: 10.1016/j.isatra.2018.12.046.

[30] H. Sai, Z. Xu, E. Zhang, C. Han, and Y. Yu, (2023) *"Chattering-free Fast Fixed-time Sliding Mode Control for Uncertain Robotic Manipulators"* **International Journal of Control, Automation and Systems** ***21***(2): 630–644. DOI: 10.1007/S12555-021-0823-4.

[31] Y. Su, C. Zheng, and P. Mercorelli, (2020) *"Robust approximate fixed-time tracking control for uncertain robot manipulators"* **Mechanical Systems and Signal Processing** ***135***: 106379. DOI: 10.1016/j.ymssp.2019.106379.

[32] X. Liu and H. Sheng, (2022) *"Active Fault Tolerant Control of Uncertain Robotic System Based on Observer and Sliding Mode"* **IFAC-PapersOnLine** ***55***(1): 598–603. DOI: 10.1016/J.IFACOL.2022.04.098.

[33] M.-D. Tran, H.-J. Kang, et al., (2015) *"Nonsingular terminal sliding mode control of uncertain second-order nonlinear systems"* **Mathematical Problems in Engineering** ***2015***: DOI: 10.1155/2015/181737.

[34] B. Ren, Y. Wang, and J. Chen, (2019) *"A novel robust finite-time trajectory control with the high-order sliding mode for human–robot cooperation"* **IEEE Access** ***7***: 130874–130882. DOI: 10.1109/ACCESS.2019.2940321.

[35] H. Sai, Z. Xu, S. He, E. Zhang, and L. Zhu, (2022) *"Adaptive nonsingular fixed-time sliding mode control for uncertain robotic manipulators under actuator saturation"* **ISA Transactions** ***123***: 46–60. DOI: 10.1016/J.ISATRA.2021.05.011.